2020

Auxin efflux controls orderly nucellar degeneration and expansion of the female gametophyte in Arabidopsis

Junzhe Wang

Xiaolong Guo

Qiang Xiao

Jianchu Zhu

Alice Y. Cheung

See next page for additional authors

Authors

Junzhe Wang, Xiaolong Guo, Qiang Xiao, Jianchu Zhu, Alice Y. Cheung, Li Yuan, Elizabeth Vierling, and Shengbao Xu

Auxin efflux controls orderly nucellar degeneration and expansion of the female gametophyte in Arabidopsis

Junzhe Wang[1][†] (iD)**, Xiaolong Guo[1][†]** (iD)**, Qiang Xiao[1]** (iD)**, Jianchu Zhu[1], Alice Y. Cheung[2]** (iD)**, Li Yuan[3]*** (iD)**, Elizabeth Vierling[2]*** (iD) **and Shengbao Xu[1,2,4]** (iD)

[1]State Key Laboratory of Crop Stress Biology for Arid Areas, College of Agronomy, Northwest A&F University, Yangling, Shaanxi 712100, China; [2]Department of Biochemistry and Molecular Biology, University of Massachusetts, Amherst, MA 01003, USA; [3]State Key Laboratory of Crop Stress Biology for Arid Areas, College of Horticulture, Northwest A&F University, Yangling, Shaanxi 712100, China; [4]Ministry of Education Key Laboratory of Cell Activities and Stress Adaptations, School of Life Sciences, Lanzhou University, Lanzhou, Gansu 730000, China

Summary

- The nucellus tissue in flowering plants provides nutrition for the development of the female gametophyte (FG) and young embryo. The nucellus degenerates as the FG develops, but the mechanism controlling the coupled process of nucellar degeneration and FG expansion remains largely unknown.
- The degeneration process of the nucellus and spatiotemporal auxin distribution in the developing ovule before fertilization were investigated in *Arabidopsis thaliana*.
- Nucellar degeneration before fertilization occurs through vacuolar cell death and in an ordered degeneration fashion. This sequential nucellar degeneration is controlled by the signalling molecule auxin.
- Auxin efflux plays the core role in precisely controlling the spatiotemporal pattern of auxin distribution in the nucellus surrounding the FG. The auxin efflux carrier PIN1 transports maternal auxin into the nucellus while PIN3/PIN4/PIN7 further delivers auxin to degenerating nucellar cells and concurrently controls FG central vacuole expansion. Notably, auxin concentration and auxin efflux are controlled by the maternal tissues, acting as a key communication from maternal to filial tissue.

Introduction

The nucellus is one of the three major functional regions of a developing ovule (Lu & Magnani, 2018). A cell in the nucellus differentiates into the megaspore mother cell (MMC), which then undergoes meiosis to yield four haploid megaspores. One of the surviving four megaspores undergoes megagametogenesis (three rounds of mitosis followed by nuclear migration and cellularization) to give rise to the mature female gametophyte (FG). Megagametogenesis in *Arabidopsis thaliana* is divided into seven stages defined by the number and position of nuclei in the developing FG. The fully differentiated FG, which takes about 50 h after meiosis to develop in *A. thaliana* (Smyth *et al.*, 1990; Christensen *et al.*, 1997), is the site of the double fertilization of the egg and the central cell, resulting in formation of the embryo and endosperm and ultimately the seed. During establishment of the FG, most nucellar cells degenerate to provide space for the expanding FG (Lu & Magnani, 2018).

Cell degeneration, in the form of programmed cell death (PCD), is common in the development of multicellular organisms, allowing unwanted cells to be replaced by new cells to form new tissues or organs (Beers, 1997; Wu & Cheung, 2000). Orderly degeneration of the remaining nucellus after fertilization has been documented in *A. thaliana* (Xu *et al.*, 2016) and rice (Yin & Xue, 2012). However, the process of nucellar degeneration before fertilization during FG development remains unexplored (Lu & Magnani, 2018), and its underlying regulatory mechanisms thus are largely unknown.

Previous studies have suggested that auxin participates in nucellar degeneration in fertilized rice ovules (Yin & Xue, 2012; Lu & Magnani, 2018), although the precise role of auxin in nucellar degeneration remains elusive. In developing *A. thaliana* ovules, the DR5 reporter system has revealed a dynamic auxin response in the nucellus around the developing FG (Benková *et al.*, 2003; Ceccato *et al.*, 2013; Lituiev *et al.*, 2013), indicating that auxin may also participate in nucellar degeneration during FG development. This dynamic auxin response in the developing ovule is proposed to be due to both local auxin biosynthesis (Cheng *et al.*, 2006; Larsson *et al.*, 2017) and polar auxin

transport (Benková *et al.*, 2003; Bencivenga *et al.*, 2012). However, expression of auxin synthesis genes (*TRYPTOPHAN AMINOTRANSFERASE OF ARABIDOPSIS 1 – TAA1* and *YUCCAs*) has not been reported in the nucellus of the developing ovule (Cheng *et al.*, 2006; Larsson *et al.*, 2017). The auxin efflux carrier protein PIN-FORMED 1 (PIN1) (Christensen *et al.*, 1997; Benková *et al.*, 2003; Bencivenga *et al.*, 2012; Ceccato *et al.*, 2013) and the auxin influx carrier LIKE AUXIN RESISTANT 1 (LAX1) (Panoli *et al.*, 2015) were detected in the nucellus, indicating that auxin transport may be responsible for dynamic auxin distribution in the nucellus. In addition, in the absence of these auxin transporters, arrested FG can be observed (Ceccato *et al.*, 2013; Panoli *et al.*, 2015), indicating that auxin transport in the nucellus plays a critical role in FG development. Still, how auxin distribution is controlled in the developing ovule is a missing piece in our current understanding of mechanisms coordinating development between the FG and surrounding maternal tissue.

Here, we address the role of auxin in the control of nucellar degeneration during FG development. We show that auxin cellular efflux plays a major role in the dynamic distribution of auxin in the nucellus during *A. thaliana* FG development, and is required for orderly nucellar degeneration and FG expansion. We found that distal maternal auxin is transported into the nucellus by the auxin efflux carrier PIN1, and that auxin is further distributed in the nucellus surrounding the FG by PIN3, PIN4 and PIN7 to establish the order of nucellar degeneration, and to allow for expansion of the FG central vacuole.

Materials and Methods

Materials

The genes evaluated in this study include auxin signalling *TRANSPORT INHIBITOR RESPONSE 1* (*TIR1*, AT3G62980) and *AUXIN RESPONSE FACTOR 6* (*ARF6*, AT1G30330), auxin efflux carriers *PIN-FORMED 1* (*PIN1*, AT1G73590), *PIN-FORMED 2* (*PIN2*, AT5G57090), *PIN-FORMED 3* (*PIN3*, AT1G70940), *PIN-FORMED 4* (*PIN4*, AT2G01420) and *PIN-FORMED 7* (*PIN7*, AT1G23080).

The following previously described transgenic and mutant lines were used in this study: *CDCpro-NLS:Mcherry* (Panoli *et al.*, 2015), *DR5rev:GFP*, *PIN1pro:PIN1-GFP*, *PIN2pro:PIN2-GFP* and *PIN3pro:PIN3-GFP* (Huang *et al.*, 2014), *PIN4pro:PIN4-GFP* and *PIN7pro:PIN7-GFP* (Blilou *et al.*, 2005), the PIN triple mutant *pin3pin4pin7* (Ding & Friml, 2010), and the partial loss-of-function PIN1 mutant *pin1-5* (Bennett *et al.*, 1995). Single and double mutants of PIIN3/PIN4/PIN7 were isolated by hybridization of PIN3/PIN4/PIN7 with Col. Complementary plants was constructed by transfer of *PIN3pro:PIN3-GFP*, *PIN4pro:PIN4-GFP* and *PIN7pro:PIN7-GFP* to the *pin347* triple mutant, respectively. These lines were verified with PCR sequencing, and genotyping with the primers in the following experiments. Primers for *pin3-5* (the *pin3* in *pin347*, T-DNA insertion line): *pin3-5LP*: CCCATCCCCAAAAGTAGAGTG; *pin3-5RP*: ATGATACACTGGAGGACGACG; *LBb1.3*: ATT

TTGCCGATTTCGGAAC. For *pin4* (the *pin4* in *pin347*, 8-bp deletion line), *gPIN4F-3105*: TCTAAGCACTGGGTAAGTTC; *gPIN4R-3259*: CAGAGTTATAGGTAAGGCTA. For *pin7-1* (the *pin7* in *pin347*, DS5 transposon insertion line), *pin7-F*: AAATCCGATCAAGGCGGTG; *pin7-R*: CGTCGAATT TCCGCAAGC; *ds5*: ACGGTCGGGAAACTAGCTCTA. For *pin1-5* (point mutation, C168T): *BsmAI-F*: CGTTTCGTCGC TCTCTTCGCCGTTCCTCTCGTCT; *pin1-5-R*: CAACGAT TTGAACCATGAGGTC. The auxin reporter DII-VENUS and the auxin response mutant *tir1-10* (SALK_090445C) were obtained from the European Arabidopsis Stock Centre (UK) and Arabidopsis Biological Resource Center (USA), respectively. The *pin1* cosuppression and ARF6 overexpression lines driven by the 35S promoter were transformed into Col wild type. Constructs were Gateway cloned into the binary vector pBIB-Basta-GWR (Gou *et al.*, 2010) with LR Clonase II (Invitrogen), after which the sequence and expression were confirmed.

Growth conditions and chemical treatments

Arabidopsis thaliana plants were grown in peat in growth chambers with a 16 h daylength (light intensity, 150 $\mu mol\,m^{-2}\,s^{-1}$) and a 21°C : 19°C, day : night temperature cycle, as described by Xu *et al.* (2013). Inflorescences containing young floral buds at different developmental stages were immersed in a solution of 100 μM *N*-1-naphthylphthalamic acid (NPA) or brefeldin A (BFA) or 50 μM NAA or 2,4-dichlorophenoxyacetic acid (2,4-D) in 0.01% Silwet L-77 (Sigma) or a mock solution of 0.01% Silwet L-77 as previously described (Nole-Wilson *et al.*, 2010). Buds were immersed for 5 min every 6–8 h for 36 h to maintain the effect of the chemicals. During this treatment period, pistils were collected at 4 h (with one treatment), 8 h (two treatments) and 24 h (four treatments) to determine the auxin response and distribution. Generally, similar alterations in auxin distribution were observed with different times of treatment, but 8 h showed the most stable patterns, and thus the 8 h treatment was selected for replications and analysis. Pistils were collected at 36 h (six treatments) for confocal laser scanning microscopy (CLSM) and aniline blue staining.

Microscopy

For aniline blue staining pistil tissue was submerged in *c*. 250 μl of acetic acid and fixed for at least 3 h, and the tissue was softened by submersion in 1 M NaOH overnight and then washed three times with 50 mM KPO_4 buffer (50 mM KPO_4 buffer (pH 7.5) prepared with 4.17 ml of 1 M K_2HPO_4 and 0.83 ml of 1 M KH_2PO_4). The tissue was stained with 200 μl aniline blue (0.01-% aniline blue in 50 mM KPO_4 buffer) for between 2 and 12 h, and then mounted on a microscope slide (Imager M2; Zeiss). Images were acquired under ultraviolet light for callose and red light for cell autofluorescence. CLSM samples were prepared according to previous reports (Christensen *et al.*, 1997; Shi *et al.*, 2005). For propidium iodide (PI) and FM4-64 stain, the carpel was dissected in a 7% glucose or 10% glycerol solution containing 0.1 mg ml^{-1} PI or 25 μg ml^{-1} FM4-64, respectively. The ovules were immersed in PI solution for 2 min and FM4-64

ovules for 10 min, and then the fluorescence signals were observed under a Leica SP8 laser confocal microscope (Figueiredo *et al.*, 2015; Li *et al.*, 2019).

Green fluorescent protein (GFP) signals for DR5::GFP were observed in ovules at flower developmental stages 12–15 with an Olympus fluorescence microscope and Olympus Fluoview FV1000, FV1100 and FV1200 confocal microscopes. For each observation, multiple non-GFP wild-type Col samples were used every 1–2 h to adjust the viewing parameters, which were then applied to GFP samples to ensure the signal is not autofluorescent background. To get stable signal from weakly expressed DII-VENUS and PIN-GFP, a Leica SP8 confocal microscope was used, and the GFP or yellow fluorescent protein (YFP) signal was collected by an HyD detector in counting mode. IMAGEJ V1.48 was used to collect PIN-GFP localization and to adjust the DR5::GFP/DII-VENUS signal to the same parameters used for the comparisons, and also to measure the length of the nucellus and central vacuole area of the ovule.

The length of the nucellar cap (Ncap) was measured from the first Ncap cell at the micropylar end, then along the Ncap cells to the last Ncap cells at the chalazal end, where a cell has converged the nucellus and the inner integuments, as shown in the gynobasal purple dash line in Fig. 1(a). The length of the nucellar base (Nbase) was measured from the centre of the Nbase at the micropylar side to the chalazal end, as shown with white lines in Fig. 1(a). The projected width of the central vacuole was measured from the section perpendicular to the proximal–distal direction with 0.5 μm step size for one slide using a ×60 oil immersion lens, and counting the number of steps from the first slide (vacuole appearance) to the last slide (vacuole disappearance) to calculate the projected vacuole width. The area of the central vacuole was measured by IMAGEJ V1.48 on the CLSM image. The volume of the central vacuole was estimated by volume = area × width × ½.

Statistical analysis

For the Nbase length and Ncap length measurements, three bulk populations of *A. thaliana* plants were observed. At least 15 clear CLSM images were acquired from each genotype, treatment and developmental stage. At least 150 ovule images with aniline blue staining for each genotype and treatment were observed. A Student *t*-test was performed in Microsoft EXCEL 2010, using two-tailed and unequal variances to evaluate the significant difference between genotypes or treatments.

Results

Degeneration of the nucellus is a highly ordered process before fertilization

With CLSM (Fig. 1a), and PI (Supporting Information Fig. S1) and aniline blue staining (Fig. S2), we examined the fate of nucellar cells during FG development in *A. thaliana*. To describe the degeneration process more precisely, we classified the nucellar tissue into three types based on the position of the nucellar cells in relation to the FG, with reference to the nomenclature of Lu & Magnani

(2018). The nucellar pad (Npad) directly surrounds the FG (blue in Fig. 1b), the Ncap is the outer layer of the nucellus that is in direct contact with inner integument cells (pink in Fig. 1b) and the Nbase is the region situated close to the chalaza (grey in Fig. 1b).

In FG1–2 stage ovules, when functional megaspore expansion and shrinkage of the degenerating megaspores is occurring, Npad cells on the micropylar end were vacuolated (green arrowheads in Fig. 1a). These vacuolated Npad cells were eliminated at the micropylar end in FG3 ovules. In conjunction with this elimination, additional Npad cells towards the chalazal end became vacuolated, suggesting Npad degeneration progresses in an orderly fashion towards the chalazal end. The pattern of cell degeneration of the Ncap started at the micropylar end during FG3–4 (yellow arrowheads in Fig. 1a) and proceeded in a chalazal direction in the following developmental stages. This sequential degeneration from micropylar to chalazal direction was further supported by PI and aniline blue staining (Figs S1, S2).

These observations demonstrate that nucellar cells undergoing degeneration during FG development first experience vacuolation (green arrowheads in Fig. 1a), then appear as deformed cell remnants (red asterisks in Fig. 1a) and finally are eliminated from the ovule (Fig. 1a,b). The cell remnants are the dead cells as shown by PI staining (white arrowheads in Fig. 1a and asterisks in Fig. S1). Nucellar degeneration can therefore be described as three successive steps: vacuolation, cell death and elimination. Additionally, the length of the Ncap decreased dramatically from FG5 to FG7 (Fig. 1c), indicating that Ncap degeneration mainly occurred during these stages and that the length of the Ncap is a reliable indicator of Ncap degeneration. By contrast, the length of the Nbase remained essentially constant during FG development (Fig. 1d).

Nucellar cells undergoing degeneration also showed maximum auxin response

The vacuolation of nucellar tissues appeared to correspond to cells that show a high auxin response in a previous study (Lituiev *et al.*, 2013). We used DR5::GFP as a marker to confirm the correlation between nucellar degeneration and auxin response in developing ovules, and the marker *CDCpro-NLS:Mcherry* (Panoli *et al.*, 2015) to simultaneously visualize dividing nuclei of the FG (Fig. 2a). In FG1 ovules, the highest auxin response was evident in the tip of the Ncap at the micropylar end of the ovule in addition to the provascular tissue of the funiculus (Fig. 2a). Increased levels of auxin activity were detected in the degenerating megaspores and adjacent Npad starting at FG2. The highest auxin response persisted in the Ncap at the micropylar end, degenerating parts of the Npad and the degenerating megaspores in FG3 ovules. This auxin response pattern is consistent with previous investigations (Pagnussat *et al.*, 2009; Lituiev *et al.*, 2013), and generally correlates with the vacuolating nucellus cells (white asterisks in Fig. 2a). Notably, after FG4 and until fertilization, the highest DR5::GFP signal was still seen in the Ncap at the micropylar end until fertilization, exactly paralleling the vacuolation of these cells (Fig. 1a,b), and which is consistent with the expression location of AtCEP1, the initiator of PCD in the nucellus (Zhou *et al.*, 2016), indicating that the high auxin
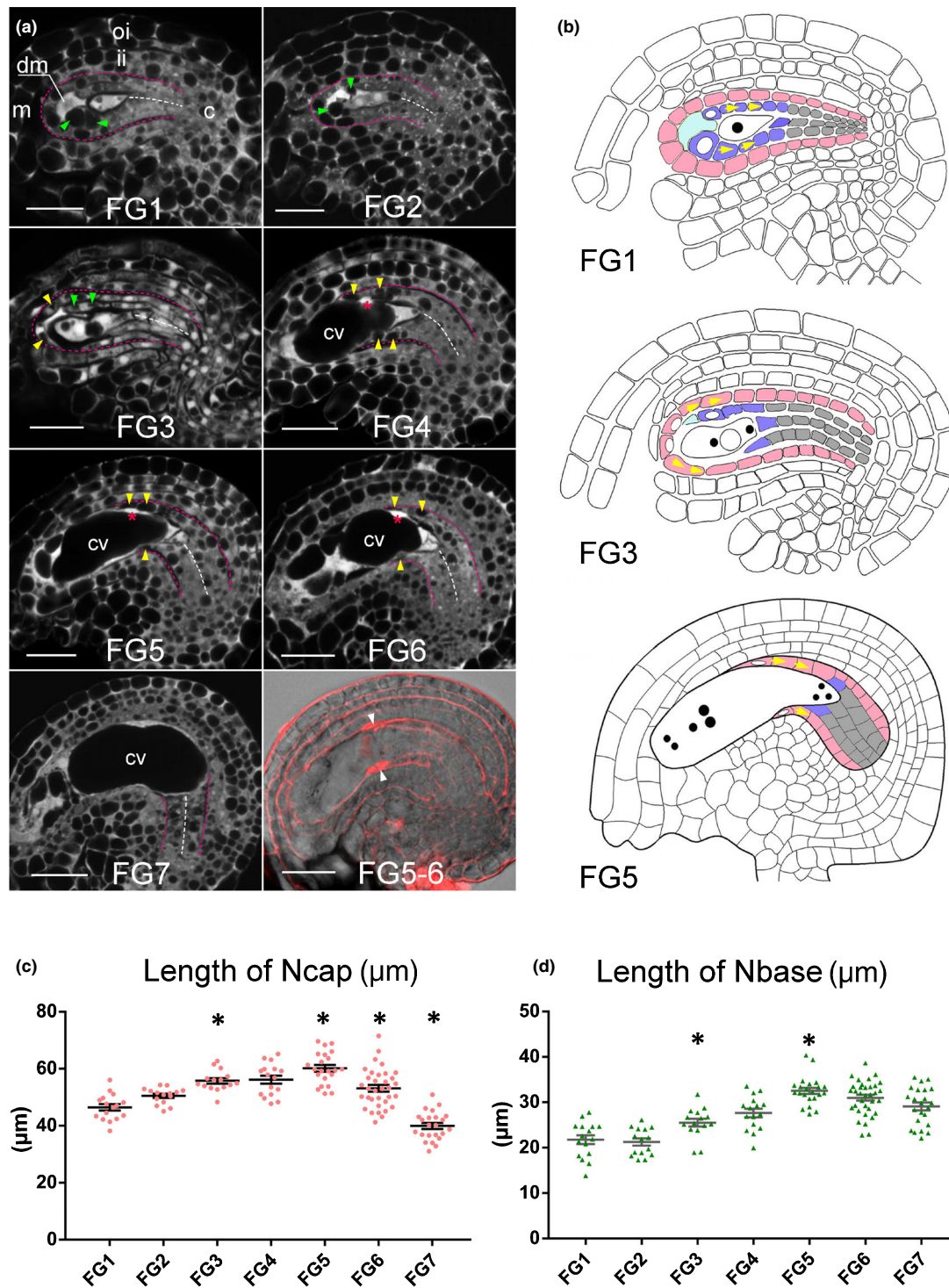
Fig. 1 Nucellar development and degeneration during Arabidopsis female gametophyte (FG) development. (a) CLSM images of nucellar degeneration during FG development. Green arrowheads indicate vacuoles in degenerating Npad cells. Yellow arrowheads indicate vacuoles in degenerating Ncap cells. Red asterisks mark collapsed remnants of degenerated nucellar cells. The purple and white lines indicate the length and position of the Ncap and Nbase, respectively. oi, outer integuments; ii, inner integuments; m, micropyle; dm, degenerating megaspores; cv, central vacuole. Bars, 20 μm. Ovule at FG5–6 is also shown after PI staining to demonstrate that the collapsed remnants are dead cells (white arrowheads). (b) Diagram of nucellar degeneration. Ncap is coloured pink, Npad is blue, Nbase is grey and the degenerating megaspores are cyan. White ellipses indicate the vacuole in the degenerating nucellar cells at each stage; the order of degeneration follows the direction of the yellow arrowheads. (c) The length of the Ncap at FG developmental stages 1 to 7. The gynobasal side of the Ncap (gynobasal purple lines in (a)) was measured with IMAGEJ. Data are means ± SE ($n \geq 15$ as shown). Asterisks indicate a significant difference in Ncap length between the indicated stage and previous stage (t-test, $P < 0.01$). (d) The length of the Nbase at FG developmental stages 1 to 7. The Nbase (white dashed lines in (a)) was measured with IMAGEJ. Data are means ± SE ($n \geq 15$ as shown). Asterisks indicate a significant difference in Nbase length between the indicated stage and previous stage (t-test, $P < 0.01$).

response is associated with nucellar cell vacuolation and the cell death programme.

We further examined the auxin reporter DII-VENUS, which produces a signal inversely proportional to auxin concentration, and can therefore be used to monitor low auxin concentrations (Brunoud *et al.*, 2012). Consistent with our DR5::GFP results, DII-VENUS signal was nearly absent in the degenerating nucellar cells (white arrowheads in Fig. 2b), supporting that degenerating nucellar cells contain a high auxin content. PI stain showed that the appearance of dead nucellar cells generally followed the auxin accumulation both in Npad and Ncap (Fig. 2c), further supporting that auxin
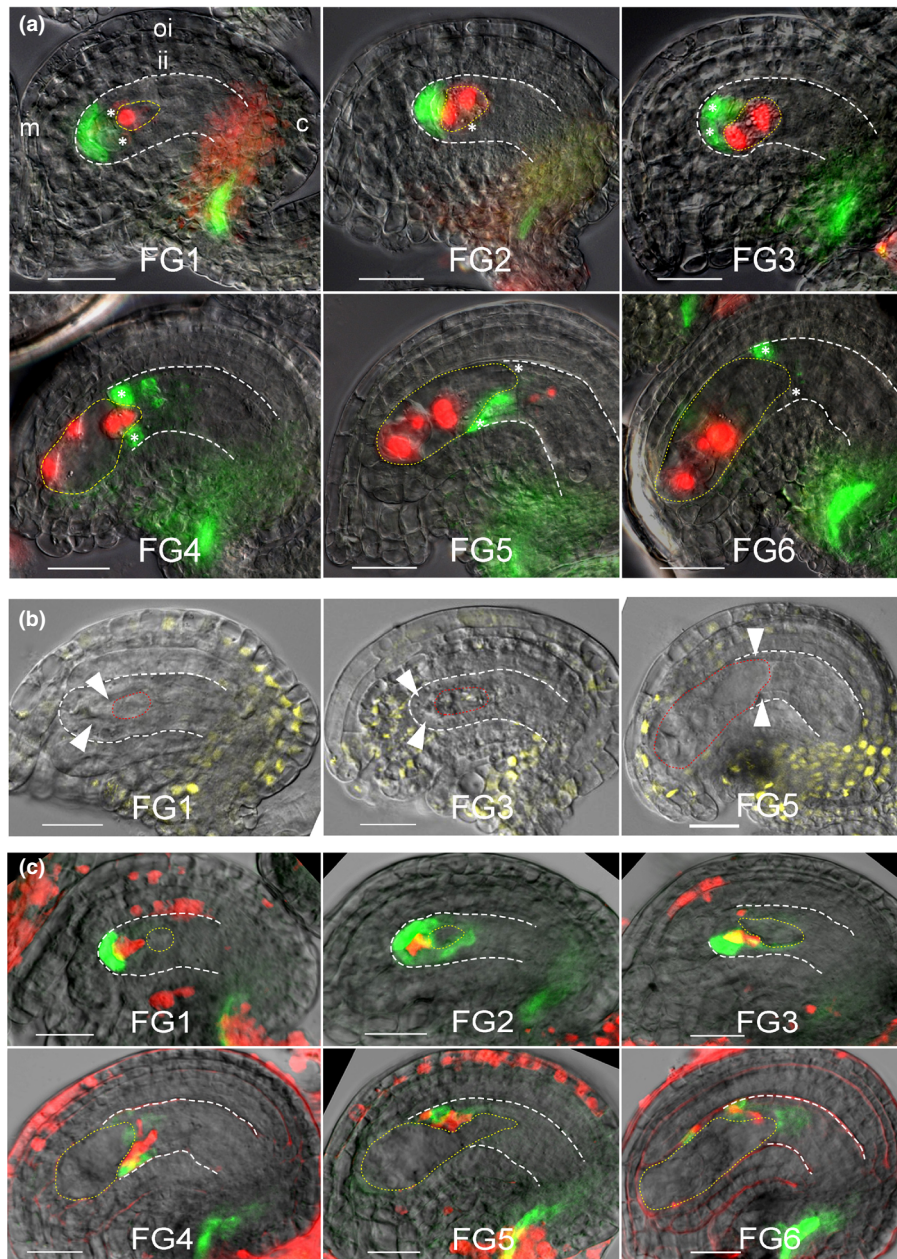
Fig. 2 Auxin distribution in the developing ovule. (a) Transcriptional response to auxin detected with DR5::GFP (green). Nuclei of Arabidopsis FG are shown by the marker *CDCpro-NLS:Mcherry* (red). The DR5::GFP signal is the strongest in the micropylar Ncap at FG1 and increases in the degenerating megaspores and adjacent Npad tissue during FG2–3. After FG4, the GFP signal remains at the micropylar end of the Ncap (which is adjacent to the FG) after the degenerating megaspores and Npad degenerated, and the high auxin response moves in the chalazal direction with FG expansion. White asterisks mark the vacuolating nucellar cells based on observations in Fig. 1. White dashed lines outline the outer edge of the Ncap and red dashed lines encircle the developing FG. oi, outer integuments; ii, inner integuments; m, micropyle; c, chalaza. Bars, 20 µm. (b) The yellow DII-VENUS signal indicates low auxin levels in specific parts of developing ovules. White arrowheads point to the absence of DII-VENUS signal in degenerating nucellar cells at the indicated FG development stage, which shows a high auxin content in these cells. Red dashed lines encircle the developing FG. Bars, 20 µm. (c) The red PI staining indicates dead cells and the green DR5-GFP indicates cells with high auxin response. Several cells staining yellow suggest that dying nucellus cells still have a relatively high auxin response. Bar, 20 µm.

accumulation is associated with the cell death programme before nucellar cell destruction.

Auxin efflux links auxin distribution and patterning of nucellar degeneration

To evaluate further the role of auxin in nucellar degeneration, we first examined degeneration of the Ncap in *tir1-10* (*TRANSPORT INHIBITOR RESPONSE 1*), which shows reduced auxin sensing, and in transgenic plants expressing *35S:: ARF6*, which have increased expression of the auxin signalling transcription factor *ARF6* (*AUXIN RESPONSE FACTOR 6*). Ovule development was investigated by CLSM at flower developmental stage 14, which corresponds to just opening flowers with ovules at FG5–7 (Smyth *et al.*, 1990). We found that Ncap length is significantly longer in FG7 stages of *tir1-10* ovules, but significantly shorter in *35S::ARF6* (ARF6-OX) ovules at FG6 and FG7 stages compared to Col wild-type ovules (Figs 3a, S3, S4), indicating that Ncap degeneration is delayed in *tir1-10* but accelerated in *35S::ARF6* ovules, and pointing to a role for both auxin and auxin signalling in Ncap degeneration.

As an additional approach to defining the importance of auxin in nucellar degeneration, flowers at different developmental stages were treated for 8 h with a synthetic auxin, the influx substrate 2,4-D (see the Materials and Methods section). Treated flowers showed a disrupted pattern of auxin response in the nucellus, exhibiting an increased response in the micropylar Nbase cells (white arrowheads in Fig. 3b). However, with long-term treatment (36 h), the increased auxin response elicited by 2,4-D did not accelerate the degeneration of Ncap as assessed by Ncap length measurement (Figs 3c, S5). By contrast, the auxin efflux substrate 1-naphthaleneacetic acid (NAA) did not disrupt the auxin distribution pattern, but specifically increased the auxin response in remnants of degenerating nucellar cells (white arrowhead in Fig. 3b) and accelerated degeneration of Ncap cells in FG5 and FG6 ovules (Figs 3c, S6). These results suggest that auxin efflux is responsible for maintaining the auxin distribution pattern in the nucellus and is involved in nucellar degeneration.

To confirm the importance of auxin efflux in nucellar cell degeneration, Arabidopsis buds at different stages were treated with two auxin efflux inhibitors: NPA and the vesicle-trafficking inhibitor BFA (Friml *et al.*, 2003; Petrasek *et al.*, 2006). After 8 h of NPA treatment, the auxin response decreased in the nucellus in the early stages of development (FG1–3, Figs 3b, S7). In addition, specific localization of auxin was lost in the degenerating Ncap of ovules in late stages of development (FG4–7). With long-term NPA treatment (36 h), the FG in *c.* 12% of ovules had collapsed or was stalled at early FG development (< FG4) in stage 14 flowers. Surrounding the collapsed FG, most Ncap cells remained, showing protoplast shrinkage (blue arrowheads) and absence of the large vacuole typical of degenerating nucellar cells (yellow arrowheads marked in control and auxin treatment samples in Fig. 3b). Protoplast shrinkage was also commonly observed at positions of degenerating nucellar cells in FG6 ovules with long-term NPA treatment (Fig. 3b). Statistical analysis showed that Ncap degeneration in FG7 ovules was severely inhibited by NPA treatment (Figs 3c, S7). Similarly, ovules treated with BFA showed a decreased auxin response in the nucellus, along with the appearance of shrunken protoplasts (blue arrowheads in Fig. 3b) and the inhibition of Ncap degeneration (Figs 3c, S8). These results strongly supported that auxin efflux links the dynamic spatiotemporal distribution of auxin, which controls nucellar degeneration.

Expression of auxin efflux carriers is consistent with auxin distribution in the nucellus

The PIN-FORMED proteins play a major role in auxin efflux in plants (Sauer & Kleine-Vehn, 2019). To understand auxin efflux in developing ovules, five PIN genes (PIN1, 2, 3, 4 and 7) were translationally fused with GFP and examined in developing ovules. PIN1 was expressed in the Ncap and provascular tissues of ovules through FG1 to FG7 (Figs 4, S9), consistent with the strong auxin response in Ncap and provascular tissue (Fig. 2a). PIN1 was also detected in Npad cells from FG3 (yellow arrowheads) and evidently expressed after FG4 at the chalazal end of the Nbase (yellow hollow arrowhead in Fig. 4).

A weak PIN2 signal was detected in the primordia of the integument at FG0, and stable expression was not detected at later stages of ovule development and was not investigated further. PIN3, PIN4 and PIN7 were detected in the degenerating megaspores (white arrowheads) and in the Npad and Nbase in developing ovules (Figs 4, S10). They were also expressed in the Ncap at the micropylar side in late developing ovules (FG4–7) when elimination of the degenerating megaspores and Npad was complete. Thus, the function of PIN3, PIN4 and PIN7 in auxin transport may be redundant in the Npad and Nbase. PIN3 was also detected in the Ncap at FG1 and in provascular cells of the chalaza and funiculus from FG3, and it gradually increased with ovule development, sharing similar localization with PIN1. Notably, all PIN3/PIN4/PIN7 localized in the interface (Fig. 4, white hollow arrowheads) between the FG and degenerating Ncap, indicating a potential auxin flux between them.

Ncap degeneration and FG expansion depend on auxin efflux

To investigate the role of these auxin efflux carriers in nucellar degeneration, ovule development in mutants of the efflux carriers *pin1* and a *pin3pin4pin7* triple mutant was assessed. In *pin1-5*, a weak allele of *PIN1*, shrunken Ncap cells without vacuoles were observed (blue arrowheads in Fig. 5a), and the Ncap in FG6–7 ovules was significantly longer than that of corresponding L*er* wild type ovules (Fig. 5b), similar to the effects of NPA and BFA treatment (Fig. 3c). Another strong *pin1* allele, a PIN1 cosuppression mutant line (*pin1-cs*) in the Col background, also showed shrunken Ncap cells and inhibited Ncap degeneration (Figs 5a,b, S10). DII-VENUS observations showed that the auxin level was significantly decreased in the degenerating Ncap in FG5–6 ovules of *pin1-cs* and Col treated by NPA, as DII-VENUS signal appeared in the degenerating Ncap (white arrowheads in Fig. 5c). These findings support the hypothesis that
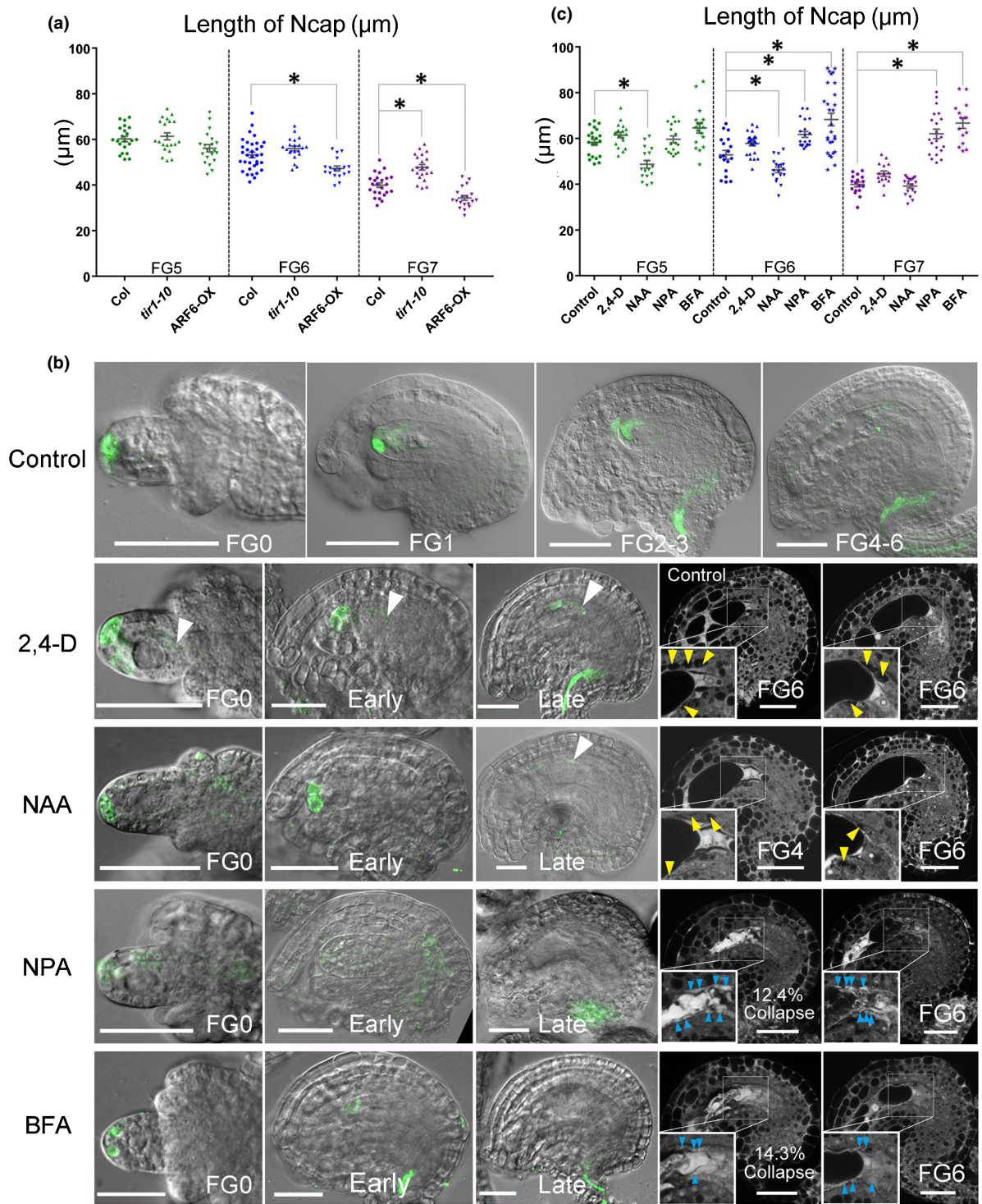
Fig. 3 Auxin efflux in ovules links auxin distribution and nucellar degeneration. (a) Length of the Ncap in *Arabidopsis* Col wild type (control), *tir1-10* mutant and *35S::ARF6* (*ARF6-OX*) transgenic line. Asterisks indicate a significant difference in Ncap length of mutants compared to wild type (Col) at the indicated stage of FG development (*t*-test, *P* < 0.01). Data are means ± SE (*n* ≥ 15 as shown). (b) Disruption of the auxin distribution pattern and alteration of FG development in young floral buds at different stages treated with a mock solution of 0.01% Silwet L-77 (control) or 50 μM 2,4-D, 50 μM NAA, 100 μM NPA or 100 μM BFA in 0.01% Silwet L-77 as indicated for 8 h before observation. Early includes FG1–3 stages and Late include FG 4–6 stages. The auxin response is visualized with DR5::GFP (green). White arrowheads indicate positions of high auxin activity that differ from the wild type. Yellow arrowheads indicate the orderly vacuolation of Ncap cells and blue arrowheads mark nucellar cell corpses in NPA- and BFA-treated Col wild type. Bars, 20 μm. (c) Length of the Ncap in (b). Data are means ± SE (*n* ≥ 15 as shown). Asterisks indicate a significant difference in Ncap length between a treatment and control at the indicated stage of FG development (*t*-test, *P* < 0.01).
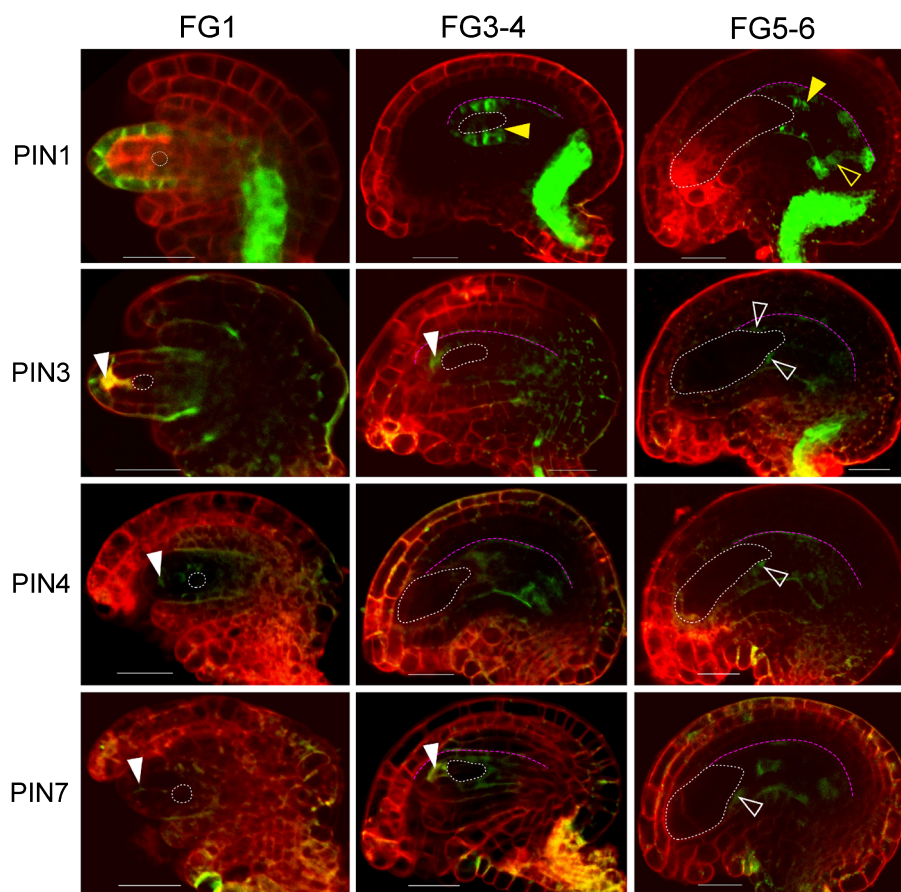
Fig. 4 PIN expression and protein localization in the developing ovule of the indicated *PINpro:PIN-GFP* plants. Representative images of PIN expression in early- (FG1), middle- (FG3–4) and late- (FG56) stage developing Arabidopsis ovules. Images were acquired with a Leica SP8 confocal microscope (see the Materials and Methods section), and the GFP signal was collected by an HyD detector with counting mode. To remove autofluorescent background, multiple non-GFP wild-type Col samples were used every 1–2 h to adjust the viewing parameters, which were then applied to GFP samples. The dye FM4-64 was applied to outline the ovule structure (red). Purple dashed lines indicate the outer edges of the gynobasal Ncap, and white dashed lines outline the developing FG. Yellow arrowheads indicate PIN1 expression in the Ncap, white arrowheads indicate PIN3, PIN4 and PIN7 in the degenerating megaspores, and white hollow arrowheads indicate PIN3 and PIN7 localized at the interface between the FG and Ncap in late developing ovules. Bars, 20 μm.

PIN1 is a major auxin efflux carrier for auxin supply during Ncap degeneration.

In the triple mutant *pin3pin4pin7* (henceforth *pin347*) (Ding & Friml, 2010), vacuoles in the degenerating Ncap were not detected (Fig. 5a). Unexpectedly, Ncap length data revealed that degeneration of the Ncap was accelerated in *pin347* (Figs 5b, S11). DII-VENUS was not detected in the degenerating Ncap (Fig. 5c) and consistently DR5::GFP showed that strong auxin activity appeared in a disorderedly degenerating Ncap (black arrowheads in Fig. 5c), supporting that Ncap degeneration depends on high auxin content, even without vacuolation. Meanwhile, this result indicates that nucellar vacuolation requires PIN3, PIN4 and PIN7 in addition to auxin supply. Furthermore, auxin also decreased in the Nbase at the chalazal end in NPA-treated Col and *pin347* (white hollow arrowheads in Fig. 5c), but not in *pin1-cs*, supporting PIN3/PIN4/PIN7 function in auxin transport in the Nbase, as their localization demonstrated (Fig. 4).

We also found that the central vacuole of the FG, which is adjacent to the degenerating nucellus, was dramatically decreased in projected width along the perpendicular axis in *pin347* compared with that of Col (Fig. 5d). Both NPA and BFA treatment reduced

the projected width of the central vacuole (Fig. 5e), indicating that central vacuole expansion in the FG requires auxin efflux. Similarly, a thinner central vacuole was observed in the *pin1* mutants (Fig. 5e). However, vacuole expansion was more inhibited in the *pin347* mutant than in the *pin1* mutant, and the effect was equal to that of the efflux inhibitors (NPA and BFA, Fig. 5e) and consistent with PIN3/PIN4/PIN7 localization (Fig. 4), suggesting that PIN3/PIN4/PIN7 plays a vital role in auxin efflux-dependent central vacuole expansion. Furthermore, single or double mutants of PIN3/PIN4/PIN7 did not show a thinner central vacuole and the accelerated Ncap degeneration (Fig. S12), and the phenotypes of *pin347* can be rescued by complementation with single PIN3, PIN4 or PIN7 (Fig. S13), strongly support the conclusion that the redundant function of PIN3, PIN4 and PIN7 is in distributing auxin in the developing ovule.

Auxin efflux is linked to Npad degeneration

To determine if degeneration of the Npad at early developmental stages is also associated with auxin efflux, ovules at FG1–3 were further investigated. We found that degenerating
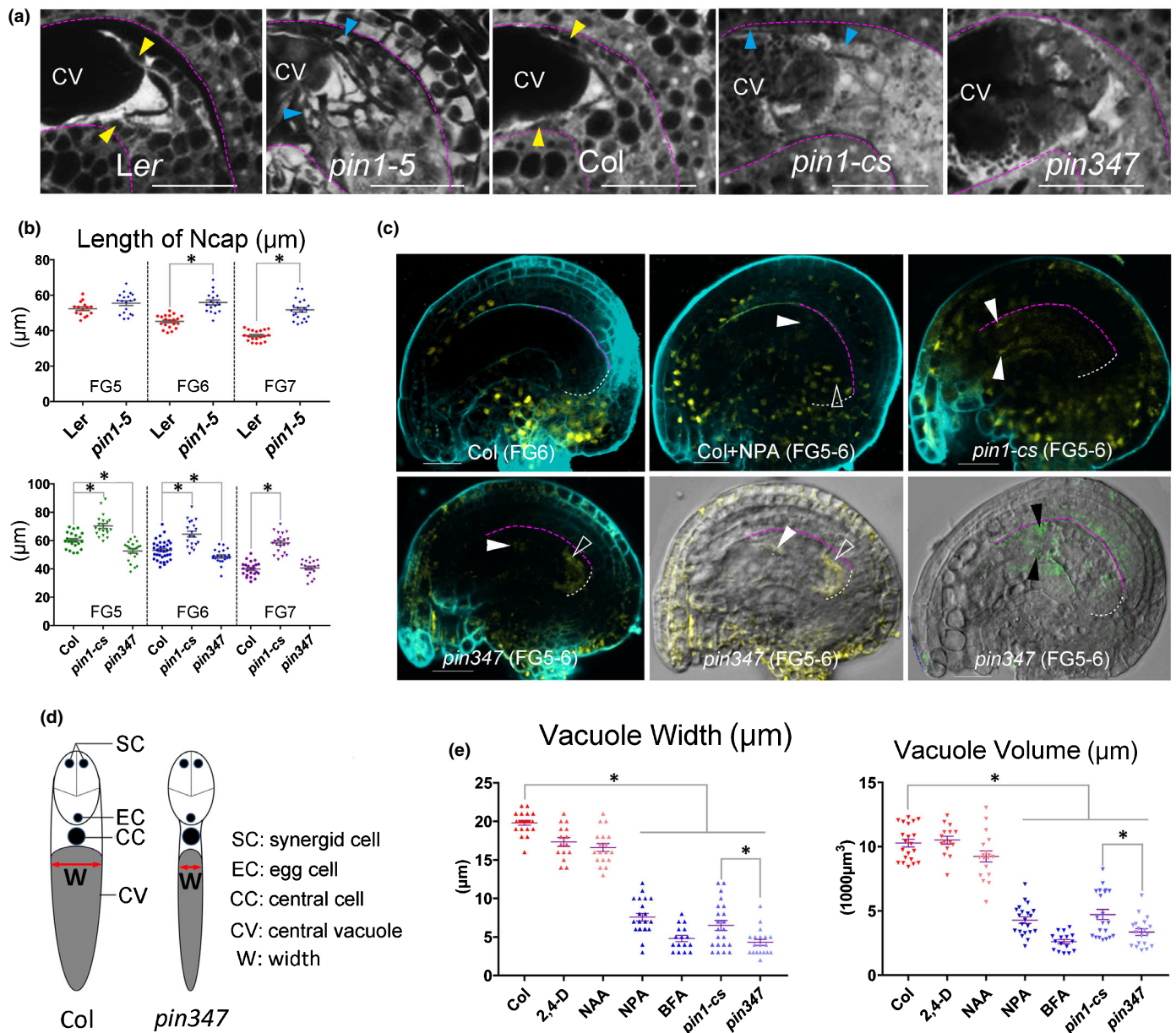
Fig. 5 Nucellar cell degeneration and FG expansion in auxin efflux mutants. (a) CLSM images showing the status of *Arabidopsis* nucellus and FG in FG6 ovules from stage 14 flowers in different auxin carrier mutants. Purple dashed lines indicate the edges of the inner integuments. The yellow arrowhead indicates the vacuole in the Ncap, blue arrowhead indicates a shrunken Ncap cells in *pin1*. Bars, 20 μm. (b) Length of the Ncap in wild type and *pin* mutants from FG5 to FG7. Data are presented as means ± SEM ($n \geq 20$). Asterisks indicate a significant difference in Ncap length of a mutant compared to wild type at the indicated stage of FG development (*t*-test, $P < 0.01$). (c) Auxin level of the nucellus in *pin* mutants and Col with or without NPA treatment. Yellow dots present the DII-VENUS signal, which results from low auxin content. Ovule structure is shown by FM4-64 dye (cyan). Green signal is from DR5::GFP. Images were acquired with a Leica SP8 confocal microscope, and the DII-VENUS/GFP signal was collected by an HyD detector with counting mode. Purple dashed lines indicate the length and position of the Ncap, and white dashed lines indicate the Nbase edge at the chalazal side. Bars, 20 μm. (d) Representative shape of the projected section of the FG at FG7 stage in Col and *pin347*. The black dots indicate the nuclei of different FG cells. The grey area indicates the FG central vacuole. (e) Width and volume of the FG central vacuole in *pin* mutants and Col with different treatments at FG7. The vacuole width was measured from the section perpendicular to the proximal–distal direction. Data are means ± SEM. At least 20 ovules at each stage were measured. Asterisks indicate a significant difference at $P < 0.01$ with a *t*-test.

Npad cells close to the degenerating megaspores were still vacuolated in FG1 ovules treated with NPA or BFA (white asterisks in Fig. 6a), suggesting that auxin influx may additionally mediate Npad auxin supply at FG1. However, vacuolation of the Npad was severely inhibited from FG2 to FG3,

and shrunken protoplasts were observed in FG3 ovules treated with NPA or BFA (Fig. 6a).

Both NAA and 2,4-D treatment significantly induced Npad vacuolation at FG1 (white asterisks in Fig. 6a). However, 2,4-D treatment did not accelerate Npad degeneration, but resulted in

shrunken protoplasts in FG3 ovules, similar to NPA and BFA treatment. By contrast, NAA induced vacuolation and degeneration, as seen by both the elimination of Npad cells and the degeneration of the micropylar Ncap in FG3 ovules (Fig. 6a). Thus, both influx and efflux appear to participate in auxin transport to the Npad, but that only auxin efflux plays the role in Npad vacuolar degeneration.

In *pin1-cs* ovules, although vacuolation was observed, the elimination of Npad cells was inhibited (Fig. 6b). By contrast, an elimination of Npad cells, with strongly inhibited vacuolation, was observed in the *pin347* mutant and more than 20% of ovules formed a large micropylar-localized FG vacuole. Shrunken protoplasts appeared in the FG3 ovule of both *pin1-cs* and *pin347*, suggesting a decreased auxin content in the degenerating Npad cells.

However, the auxin efflux substrate NAA could not rescue the inhibited Npad degeneration in *pin1-cs* (Fig. 6b). By contrast, Npad vacuolation was dramatically induced by NAA in FG1 ovules of the *pin347* mutant (Fig. 6b), strongly suggesting that PIN1 has a role in transporting distal maternal auxin into the developing ovule. After FG2, exogenous NAA failed to induce vacuolation of the Npad in *pin347*, and degeneration of the Npad surrounding the FG was disordered, with all Npad cells

degenerating simultaneously in FG2 and FG3 ovules (Fig. 6b). These results support PIN1 function in transporting auxin into the nucellus and PIN3/PIN4/PIN7 function in maintaining the vacuolation process and the order of Npad cell degeneration, the same function of PIN3/PIN4/PIN7 in the Ncap degeneration process (Fig. 5a,c).

DII-VENUS observations showed low auxin content in the degenerating megaspores, the Npad and Nbase from FG1 to FG3 in ovules and in NPA-treated ovules (Fig. 6c), but increased auxin in Nbase cells of *pin1-cs* at the micropylar end (white arrowhead) compared to NPA-treated Col. Surprisingly, DII-VENUS signal disappeared in most cells of the ovule in *pin347*, but appeared in the degenerating megaspores and the Npad surrounding the FG, suggesting PIN3/PIN4/PIN7 plays a critical role in maintaining auxin distribution in the whole ovule and transports auxin into the Npad. DR5::GFP fluorescence showed that auxin was retained in the Nbase of *pin347* at the chalazal end (Fig. 6d), confirming a role for auxin transport by PIN3/PIN4/PIN7 from the Nbase to Npad during early stage FG. However, auxin can be transported to the micropylar Nbase at the end of FG3, increasing auxin in both the Ncap and the Nbase at the micropylar end (Fig. 6d), consistent with PIN1 start expression in Npad from this stage (Fig. 4). Auxin content
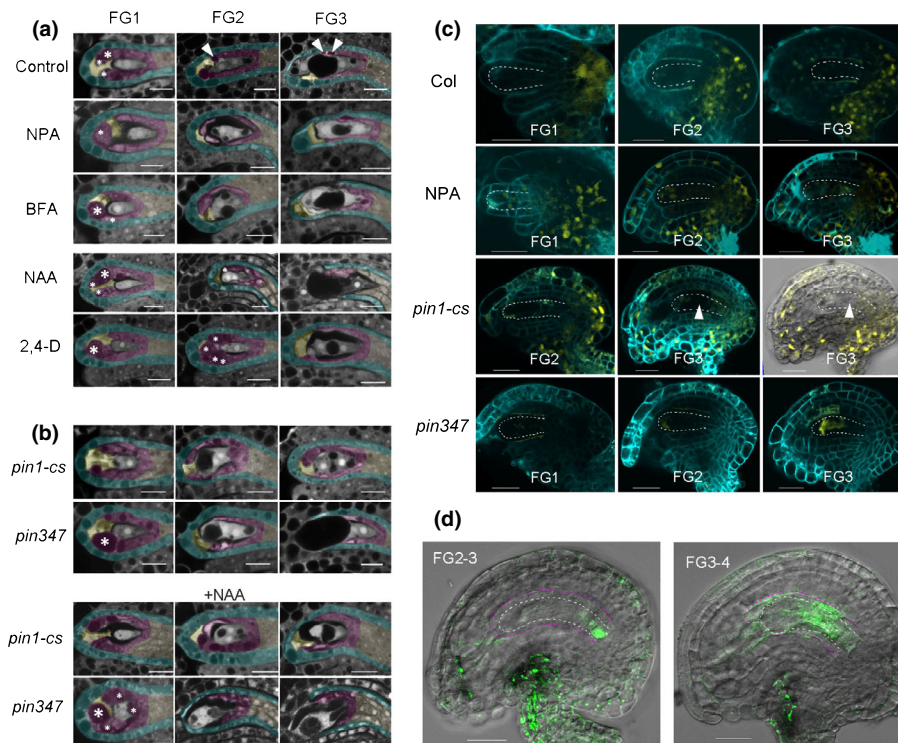

Fig. 6 Degeneration of Arabidopsis Npad is partially dependent on auxin efflux. (a) CLSM images of Npad degeneration in FG1, FG2 and FG3 ovules with chemical treatments. White asterisks indicate the vacuoles in Npad cells adjacent to the degenerating megaspores of FG1 ovules. White arrowheads in the control image indicate vacuoles in Npad cells of FG2 and FG3 ovules. Images are false coloured: cyan, Ncap; purple, Npad; pale brown, Nbase; yellow, degenerating megaspores. Bars, 10 μm. (b) Degeneration of the Npad in *pin* mutants with or without NAA treatment. Lower panel shows the degeneration of the Npad in *pin* mutants with NAA treatment. White asterisks indicate the vacuoles in the Npad. Bars, 10 μm. (c) Auxin content distribution in *pin* mutants and Col with or without NPA treatment. Images were acquired with a Leica SP8 confocal microscope, and the DII-VENUS signal was collected by an HyD detector with counting mode. Ovule structure is shown by FM4-64 dye (cyan). White dashed lines – inner edge of the Ncap. White arrowheads indicate the Nbase without DII-VENUS signal in *pin1-cs*, compared to the Col with NPA treatment. Note, the same ovule was presented in *pin1-cs* at FG3 imaged for FM4-64 and DIC respectively. Bars, 20 μm. (d) DR5::GFP in *pin347* at approximately stage FG3. Purple dashed line – outer edge of the Ncap; white dashed line, inner edge of the Ncap. Bars, 20 μm.

observations demonstrated that the spatiotemporal auxin pattern in the degenerating nucellus is closely controlled by auxin efflux (Fig. 7a), which plays the core role in regulating the degeneration process and the order of nucellar degeneration.

The role of auxin in nucellar cell death

To further clarify the precise role of auxin in nucellar degeneration, the nucellus was carefully investigated with PI staining to identify the dead cells. We found that most of the nucellus in *pin1-cs* is not the dead cells (Figs 7b, S11), although they showed a shrunken protoplast appearance (Figs 5a, 6b). Many dead cells

were observed in *pin347* (Figs 7b, S12), consistent with its accelerated cell death process, then also implying that the dead cells could not be eliminated in time. Interestingly, the dead nucellus appears in the Nbase at the chalazal end in *pin347* (white hollow arrowhead in Fig. 7b; Fig. S12), which are the auxin-enriched cells (Figs 5c, 6d), suggesting that accumulated auxin alone could result in cell death. In addition, inner integument cells showed many dead cells in *pin1-cs* (white arrowheads in Fig. 7b; Fig. S11), which usually degenerates after fertilization (Nakaune *et al.*, 2005). We therefore applied NPA to inhibit auxin efflux in Col, and found that the dying integument cells generally showed a higher auxin response (Fig. 7c), as dead nucellus cells (yellow
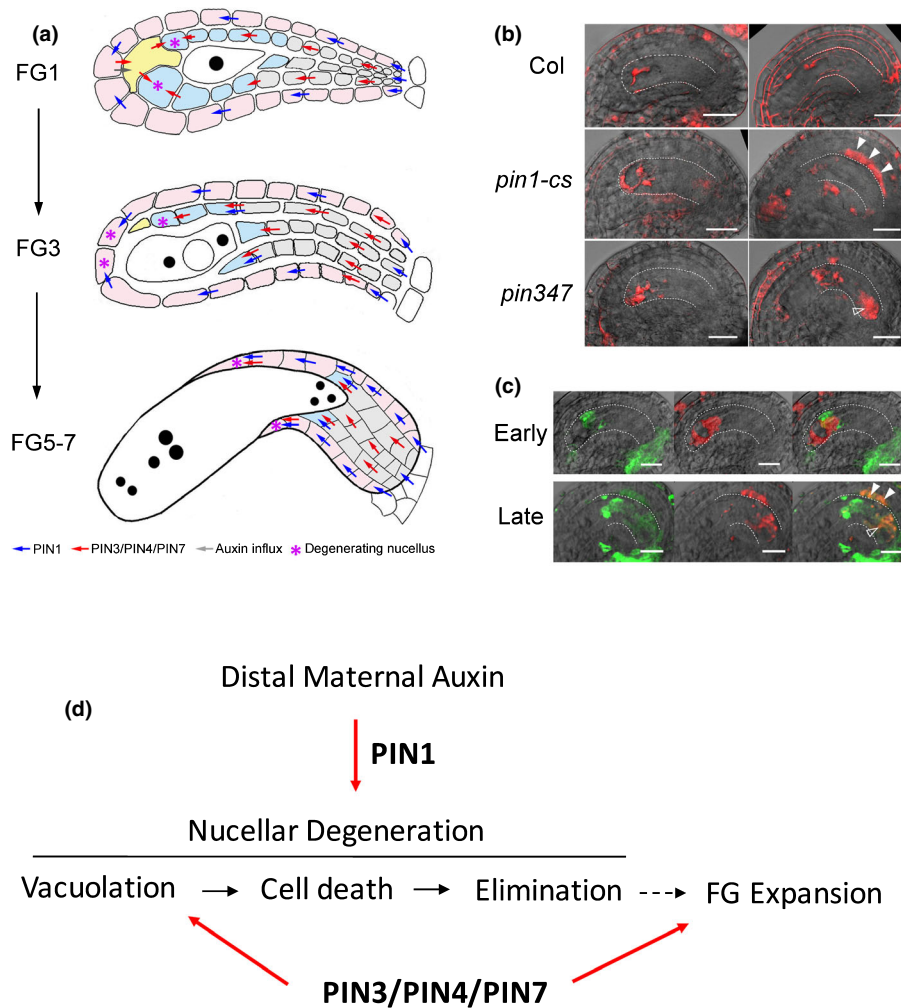
Fig. 7 Auxin efflux in Arabidopsis nucellar degeneration. (a) Diagram of auxin efflux in nucellar degeneration. The Ncap is pink, Npad is blue, Nbase is grey, and the degenerating megaspores are yellow. In FG1 ovules, auxin from distal maternal tissue is transported by PIN1 through the Ncap to the micropylar nucellus, and combined with locally synthesized auxin, moves to the degenerating megaspores by efflux and influx at the same time. Auxin is further transported to the adjacent degenerating Npad by PIN3/PIN4/PIN7. Meanwhile, PIN3/PIN4/PIN7 also transports auxin to the micropylar Npad from the Nbase, initiating Npad vacuolar degeneration. In FG3 ovules, auxin is mainly transported into the Npad by PIN3/PIN4/PIN7 from the Nbase, and induces orderly Npad degeneration in a chalazal direction. Late in the FG3 stage, auxin is transported into the Ncap at the micropylar end to initiate Ncap degeneration. After FG4, PIN1 is responsible for auxin flux into the micropylar terminal Ncap, continuing degeneration in a chalazal direction. Auxin homeostasis in the predegenerating and degenerating Npad and Ncap is fine-tuned by PIN3/PIN4/PIN7, which control orderly cell vacuolation and degeneration and further participate in the expansion of the FG central vacuole. (b) Cell death in developing ovule of wild type, *pin1-cs* and *pin347*. Red PI staining indicates the dead cells. White dashed line indicates the outer edge of the Ncap. White arrowheads indicate the dead integument cells and white hollow arrowhead indicates the dead nucellus in Nbase. Bars, 20 μm. (c) The dead cells in developing ovules of Col with NPA treatment. Red PI staining indicates the dead cells. White dashed line indicates the outer edge of the Ncap. The green DR5-GFP signal and red PI signal was adjusted to a high level by the IMAGEJ software to show the relative intensity. Bars, 20 μm. (d) A model of auxin efflux-dependent nucellar degeneration and FG expansion.

cells in Fig. 2c), supporting that abnormal auxin accumulation leads to cell death.

Auxin efflux is maternally controlled process

As seen with NPA and BFA treatment, a collapsed FG and early stage FG were also observed in *pin1-cs* and *pin347* in this study and previous reports (Ceccato *et al.*, 2013; Panoli *et al.*, 2015), indicating the auxin efflux also participates in FG development. Genetic tests showed that the *PIN* mutant haplotype is transmitted from FG to the next generation equally to the wild type (Table 1), suggesting that these auxin efflux carriers (PIN1, PIN3, PIN4 and PIN7) do not function in FG development directly, but rather exert an effect on FG development due to the maternal genotype, consistent with their localization (Fig. 4). This highlights that maternal auxin has a critical role in regulating orderly nucellus degeneration and normal FG development, providing a key signalling mechanism of maternal control of FG development.

In summary, our data demonstrate that distal maternal auxin was transported into the nucellus by PIN1 and further distributed in nucellus by PIN3/PIN4/PIN7 to control orderly vacuolation, cell death and elimination of dead cells, and concurrently controlling the expansion of the FG central vacuole (Fig. 7d).

Discussion

Our observations of dynamic auxin distribution and nucellar degeneration, along with synchronized FG expansion, provide fundamental clues to the mechanisms involved in auxin efflux-dependent, ordered nucellar degeneration. This study suggests that auxin participates in cell degeneration, connecting auxin efflux to cell death control, and implicating the involvement of auxin from cell initiation to cell demise, extending our understanding of auxin in plant development.

Auxin supply and spatiotemporal pattern in the developing ovule

The spatiotemporal distribution of auxin in the developing ovule plays a critical role in the coordinated development of the

Table 1 Transmission rates of Arabidopsis *pin* mutant alleles

(1)	(*pin347* × *PIN347*) × *PIN347*	*pin3*	*pin4*	*pin7*
	pin347 (+/−)	182	173	168
	PIN347 (+/+)	179	160	177
(2)	(*pin1* × *PIN1*) × *PIN1*	*pin1* (−/−)	*pin1* (+/−)	*PIN1* (+/+)
		0	121	110
(3)	F2 (*pin1* × *PIN1*)	*pin1* (−/−)	*pin1* (+/−)	*PIN1* (+/+)
		43	88	48

(1) The transmission of *PIN3*, *PIN4* and *PIN7* was tested in mutant *pin347* in Col background. (2) The transmission of *PIN1* was tested in mutant *pin1-5* in L*er* background. (3) The segregation of F₂ generation of *pin1-5* heterozygotes.

sporophyte and gametophyte (Benková *et al.*, 2003; Pagnussat *et al.*, 2009; Bencivenga *et al.*, 2011; Lituiev *et al.*, 2013). However, the mechanism underlying the spatiotemporal pattern remains largely unclear. We have demonstrated that the auxin spatiotemporal pattern is closely controlled by auxin efflux and is essential for nucellar vacuolar degeneration, elucidating an underlying function for dynamic auxin distribution in the developing ovule. Auxin efflux carriers PIN3/PIN4/PIN7 play a critical role in maintaining the auxin gradient in the whole developing ovule (Figs 5c, 6c), and PIN1 functions in transporting distal maternal auxin into the nucellus. Together, these PIN proteins precisely deliver the auxin into the degenerating nucellus (Fig. 7a). However, local auxin synthesis and auxin influx cannot be neglected, especially with regard to FG development. As we observed, fewer than 15% of FGs were inhibited at early stages of development or collapsed after long-term NPA or BFA treatment or in *pin1* mutants. This implies that local auxin synthesis in ovules along with auxin influx afford a basic auxin supply for FG development, but there is still a need for the auxin transport from distal maternal tissue. We speculate that both local and distal maternal auxin synthesis is required for the ovule and FG development, providing a critical mechanism that allows the maternal plant to control filial development in varying growth conditions.

Auxin-dependent nucellar degeneration

Unwanted cells tend to degenerate in a regulated fashion. This is seen in the degeneration of the inner integuments during plant embryo development (Nakaune *et al.*, 2005) and nucellar degeneration after fertilization in Arabidopsis and rice (Yin & Xue, 2012; Xu *et al.*, 2016). Other cell death processes include degeneration of the ephemeral endosperm (López-Fernández & Maldonado, 2016), of rice aleurone cells (Zheng *et al.*, 2017) and of Arabidopsis root cap cells (Xuan *et al.*, 2016). The underlying control and mechanisms of orderly cell degeneration, however, remain largely unknown. We found that auxin efflux perfectly integrates into the nucellar degeneration process via polar transport and provides a mechanism that directs orderly terminal cell degeneration of cells surrounding the FG. A recent study showed auxin efflux and a high auxin response in the inner integument after fertilization (Robert *et al.*, 2018), coinciding with orderly vacuolar degeneration of the inner integument (Nakaune *et al.*, 2005). Taken together with the results presented here, it appears that auxin efflux has a general role in regulating orderly vacuolar degeneration of unwanted cells surrounding a newly formed organ. In this way, the nutrition released from degenerated cells, along with the auxin, may be effectively transferred to the adjacent new organ.

Vacuolar cell death occurs during plant tissue or organ formation and elimination (van Doorn *et al.*, 2011), but there is no information about its connection to the auxin. We found that vacuolation requires auxin participation, and has to be maintained by the auxin efflux carriers PIN3/PIN4/PIN7, otherwise the nucellus will be rapidly degenerated without vacuolation, as shown in the mutant *pin347*, indicating that auxin homeostasis plays a critical role in vacuolation. We therefore speculate that

the expansion of the FG central vacuole may still depend on auxin, and has to be controlled by the maternal PIN3/PIN4/PIN7.

Interestingly, auxin alone can induce cell death (Fig. 7b), consistent with expression of the transcriptional factor MADS29, which is induced by auxin and functions in nucellar degeneration (Yin & Xue, 2012), suggesting that auxin has a general role in plant PCD. This may profoundly influence further study of PCD in plants.

The role of the FG in nucellus degeneration

Our data suggest that maternal auxin controls FG expansion by auxin supply. In most contexts, however, degenerating cells have to contact newly formed tissues to initiate the degeneration process (Gilchrist, 1998). Previous observations have shown that the nucellus fails to degenerate if FG function is impaired (Yang et al., 1999). Our observation that orderly degeneration of the nucellus begins from the nucellus adjacent to the FG indicates that the signal for degeneration may be produced by the FG, as suggested by the fact that nucellar degeneration after fertilization requires signals from the adjacent endosperm (Xu et al., 2016). Given that accumulated auxin may be sufficient to trigger cell death, signalling from the FG would amplify the cell death signal induced by auxin, as shown by our observation that the micropylar Ncap has the highest auxin response and then it dies later than the Npad at the micropylar end.

As we demonstrate, auxin efflux is the key to organizing the whole degeneration process, and thus how to set up auxin efflux is a key question. It will be important to investigate the underlying mechanism of the interaction between newly formed tissues and unwanted cells, in order to uncover the nature of this signal, and to understand how development of newly formed tissues occurs surrounding dying cells.

Author contributions

JW, XG and SX performed most transgenic work, crossing and plant material preparation. SX, JW, XG, JZ and QX performed the chemical treatments, microscopy observations and figure design. AC set up the microscopy observation protocol and quality evaluation of ovule observations. EV and SX designed the study. LY observed auxin distribution in developing ovules independently and reached similar conclusions. LY, EV and SX organized the data and wrote the manuscript. All of the authors were involved in the revision of the manuscript and approved the final manuscript. LY and EV contributed equally to this work.

ORCID

Alice Y. Cheung (ID) https://orcid.org/0000-0002-7973-022X
Xiaolong Guo (ID) https://orcid.org/0000-0001-6624-1219
Elizabeth Vierling (ID) https://orcid.org/0000-0002-0066-4881
Junzhe Wang (ID) https://orcid.org/0000-0003-2064-0585
Qiang Xiao (ID) https://orcid.org/0000-0003-4656-4314
Shengbao Xu (ID) https://orcid.org/0000-0003-2167-5341
Li Yuan (ID) https://orcid.org/0000-0003-1803-6661

References

Beers EP. 1997. Programmed cell death during plant growth and development. *Cell Death and Differentiation* 4: 649–661.

Bencivenga S, Colombo L, Masiero S. 2011. Cross talk between the sporophyte and the megagametophyte during ovule development. *Sexual Plant Reproduction* 24: 113–121.

Bencivenga S, Simonini S, Benková E, Colombo L. 2012. The transcription factors BEL1 and SPL are required for cytokinin and auxin signaling during ovule development in *Arabidopsis*. *Plant Cell* 24: 2886–2897.

Benková E, Michniewicz M, Sauer M, Teichmann T, Seifertová D, Jürgens G, Friml J. 2003. Local, efflux-dependent auxin gradients as a common module for plant organ formation. *Cell* 115: 591–602.

Bennett SRM, Alvarez J, Bossinger G, Smyth DR. 1995. Morphogenesis in pinoid mutants of *Arabidopsis thaliana*. *The Plant Journal* 8: 505–520.

Blilou I, Xu J, Wildwater M, Willemsen V, Paponov I, Friml J, Heidstra R, Aida M, Palme K, Scheres B. 2005. The PIN auxin efflux facilitator network controls growth and patterning in *Arabidopsis* roots. *Nature* 433: 39–44.

Brunoud G, Wells DM, Oliva M, Larrieu A, Mirabet V, Burrow AH, Beeckman T, Kepinski S, Traas J, Bennett MJ et al. 2012. A novel sensor to map auxin response and distribution at high spatio-temporal resolution. *Nature* 482: 103–106.

Ceccato L, Masiero S, Roy DS, Bencivenga S, Roig-Villanova I, Ditengou FA, Palme K, Simon R, Colombo L. 2013. Maternal control of PIN1 is required for female gametophyte development in Arabidopsis. *PLoS ONE* 8: e66148.

Cheng Y, Dai X, Zhao Y. 2006. Auxin biosynthesis by the YUCCA flavin monooxygenases controls the formation of floral organs and vascular tissues in *Arabidopsis*. *Genes & Development* 20: 1790–1799.

Christensen CA, King EJ, Jordan JR, Drew GN. 1997. Megagametogenesis in *Arabidopsis* wild type and the *Gf* mutant. *Sexual Plant Reproduction* 10: 49–64.

Ding Z, Friml J. 2010. Auxin regulates distal stem cell differentiation in *Arabidopsis* roots. *Proceedings of the National Academy of Sciences, USA* 107: 12046–12051.

van Doorn WG, Beers EP, Dangl JL, Franklin-Tong VE, Gallois P, Hara-Nishimura I, Jones AM, Kawai-Yamada M, Lam E, Mundy J et al. 2011. Morphological classification of plant cell deaths. *Cell Death and Differentiation* 18: 1241–1246.

Figueiredo DD, Batista RA, Roszak PJ, Köhler C. 2015. Auxin production couples endosperm development to fertilization. *Nature Plants* 1: 15184.

Friml J, Vieten A, Sauer M, Weijers D, Schwarz H, Hamann T, Offringa R, Jurgens G. 2003. Efflux-dependent auxin gradients establish the apical-basal axis of Arabidopsis. *Nature* 426: 147–153.

Gilchrist DG. 1998. Programmed cell death in plant disease: the purpose and promise of cellular suicide. *Annual Review of Phytopathology* 36: 393–414.

Gou X, He K, Yang H, Yuan T, Lin H, Clouse SD, Li J. 2010. Genome-wide cloning and sequence analysis of leucine-rich repeat receptor-like protein kinase genes in *Arabidopsis thaliana*. *BMC Genomics* 11: 19.

Huang J-b, Liu H, Chen M, Li X, Wang M, Yang Y, Wang C, Huang J, Liu G, Liu Y. 2014. ROP3 GTPase contributes to polar auxin transport and auxin

responses and is important for embryogenesis and seedling growth in *Arabidopsis*. *Plant Cell* **26**: 3501–3518.

Larsson E, Vivian-Smith A, Offringa R, Sundberg E. 2017. Auxin homeostasis in Arabidopsis ovules is anther-dependent at maturation and changes dynamically upon fertilization. *Frontiers in Plant Science* **8**: 1735.

Li H, Cai Z, Wang X, Li M, Cui Y, Cui N, Yang F, Zhu M, Zhao J, Du W *et al.* 2019. SERK receptor-like kinases control division patterns of vascular precursors and ground tissue stem cells during embryo development in Arabidopsis. *Molecular Plant* **12**: 984–1002.

Lituiev DS, Krohn NG, Muller B, Jackson D, Hellriegel B, Dresselhaus T, Grossniklaus U. 2013. Theoretical and experimental evidence indicates that there is no detectable auxin gradient in the angiosperm female gametophyte. *Development* **140**: 4544–4553.

López-Fernández MP, Maldonado S. 2016. Programmed cell death in seeds of angiosperms. *Journal of Integrative Plant Biology* **57**: 996–1002.

Lu J, Magnani E. 2018. Seed tissue and nutrient partitioning, a case for the nucellus. *Plant Reproduction* **31**: 309–317.

Nakaune S, Yamada K, Kondo M, Kato T, Tabata S, Nishimura M, Hara-Nishimura I. 2005. A vacuolar processing enzyme, deltaVPE, is involved in seed coat formation at the early stage of seed development. *Plant Cell* **17**: 876–887.

Nole-Wilson S, Azhakanandam S, Franks RG. 2010. Polar auxin transport together with *AINTEGUMENTA* and *REVOLUTA* coordinate early Arabidopsis gynoecium development. *Developmental Biology* **346**: 181–195.

Pagnussat GC, Alandete-Saez M, Bowman JL, Sundaresan V. 2009. Auxin-dependent patterning and gamete specification in the *Arabidopsis* female gametophyte. *Science* **324**: 1684–1689.

Panoli A, Martin MV, Alandete-Saez M, Simon M, Neff C, Swarup R, Bellido A, Yuan L, Pagnussat GC, Sundaresan V. 2015. Auxin import and local auxin biosynthesis are required for mitotic divisions, cell expansion and cell specification during female gametophyte development in *Arabidopsis thaliana*. *PLoS ONE* **10**: e0126164.

Petrasek J, Mravec J, Bouchard R, Blakeslee JJ, Abas M, Seifertova D, Wisniewska J, Tadele Z, Kubes M, Covanova M *et al.* 2006. PIN proteins perform a rate-limiting function in cellular auxin efflux. *Science* **312**: 914–918.

Robert HS, Park C, Gutierrez CL, Wojcikowska B, Pencik A, Novak O, Chen J, Grunewald W, Dresselhaus T, Friml J *et al.* 2018. Maternal auxin supply contributes to early embryo patterning in *Arabidopsis*. *Nature Plants* **4**: 548–553.

Sauer M, Kleine-Vehn J. 2019. PIN-FORMED and PIN-LIKES auxin transport facilitators. *Development* **146**: dev168088.

Shi DQ, Liu J, Xiang YH, Ye D, Sundaresan V, Yang WC. 2005. *SLOW WALKER1*, essential for gametogenesis in Arabidopsis, encodes a WD40 protein involved in 18S ribosomal RNA biogenesis. *Plant Cell* **17**: 2340–2354.

Smyth DR, Bowman JL, Meyerowitz EM. 1990. Early flower development in *Arabidopsis*. *Plant Cell* **2**: 755–767.

Wu HM, Cheung AY. 2000. Programmed cell death in plant reproduction. *Plant Molecular Biology* **44**: 267–281.

Xu S, Guerra D, Lee U, Vierling E. 2013. *S*-Nitrosoglutathione reductases are low-copy number, cysteine-rich proteins in plants that control multiple developmental and defense responses in Arabidopsis. *Frontiers in Plant Science* **4**: 430.

Xu W, Fiume E, Coen O, Pechoux C, Lepiniec L, Magnani E. 2016. Endosperm and nucellus develop antagonistically in Arabidopsis seeds. *Plant Cell* **28**: 1343–1360.

Xuan W, Band LR, Kumpf RP, Van Damme D, Parizot B, De Rop G, Opdenacker D, Moller BK, Skorzinski N, Njo MF *et al.* 2016. Cyclic programmed cell death stimulates hormone signaling and root development in *Arabidopsis*. *Science* **351**: 384–387.

Yang WC, Ye D, Xu J, Sundaresan V. 1999. The *SPOROCYTELESS* gene of Arabidopsis is required for initiation of sporogenesis and encodes a novel nuclear protein. *Genes & Development* **13**: 2108–2117.

Yin LL, Xue HW. 2012. The MADS29 transcription factor regulates the degradation of the nucellus and the nucellar projection during rice seed development. *Plant Cell* **24**: 1049–1065.

Zheng Y, Zhang H, Deng X, Liu J, Chen H. 2017. The relationship between vacuolation and initiation of PCD in rice (*Oryza sativa*) aleurone cells. *Scientific Reports* **7**: 41245.

Zhou LZ, Höwing T, Müller B, Hammes UZ, Gietl C, Dresselhaus T. 2016. Expression analysis of KDEL-CysEPs programmed cell death markers during reproduction in Arabidopsis. *Plant Reproduction* **29**: 265–272.

Supporting Information

Additional Supporting Information may be found online in the Supporting Information section at the end of the article.

Fig. S1 PI staining showing nucellar death process during ovule development in Col wild type.

Fig. S2 Aniline blue staining showing ovule development in Col wild type.

Fig. S3 Degeneration of the Ncap in *tir1-10* and *35S::ARF6* from FG5 to FG7.

Fig. S4 Aniline blue staining showing a callose burst in the degenerating nucellus of *tir1-10*.

Fig. S5 Aniline blue staining showing ovule development with 2,4-D treatment.

Fig. S6 Aniline blue staining showing ovule development with NAA treatment.

Fig. S7 Aniline blue and PI staining showing ovule development with NPA treatment.

Fig. S8 Aniline blue staining showing ovule development with BFA treatment.

Fig. S9 Expression of PINs in the developing ovule.

Fig. S10 Aniline blue and PI staining showing ovule development in *pin1-cs*.

Fig. S11 Aniline blue and PI staining showing ovule development in *pin347*.

Fig. S12 The variations of related parameters of nucellus cells and central vacuoles in auxin efflux mutants.

Fig. S13 The variations of related parameters of nucellus cells and central vacuoles in *pin347* mutant complementary lines.

Please note: Wiley-Blackwell are not responsible for the content or functionality of any supporting information supplied by the authors. Any queries (other than missing material) should be directed to the *New Phytologist* Central Office.